

Article

Impact of Oat Husk Extracts on Mid-Stage Cement Hydration and the Mechanical Strength of Mortar

Alysson Larsen Bonifacio *  and Paul Archbold 

Sustainable Infrastructure Research Group, Technological University of the Shannon: Midlands Midwest, N37 HD68 Athlone, Ireland; paul.archbold@tus.ie

* Correspondence: a00278550@student.tus.ie

Abstract: The valorisation of lignocellulosic resources, such as oat husks, as components in cementitious composites presents challenges regarding their compatibility with the matrix due to the solubilisation of their surface components and products from alterations induced by the alkaline environment of lime-based matrices. These negatively affect the matrix. This study aims to fill the knowledge gap regarding the compatibility and effects of the extractives found in oat husks with the cement matrix. It intends to characterise oat husks' structural composition, evaluate the extractive removal efficiency, assess their influence on cement matrix hydration using thermogravimetric techniques, and analyse mechanical strength development between 3 and 28 days. The study concludes that hot water is more efficient for extractive removal, and the immersion duration is more relevant than the number of washing cycles. Furthermore, it confirms that husks' extractives inhibit cement matrix hydration products and mechanical strength development, especially in the presence of degradation products. These findings are essential for determining more efficient approaches to enhance compatibility between oat husks and cementitious matrices.

Keywords: oat husks; cement; extractives; hydration; mechanical properties



Citation: Bonifacio, A.L.; Archbold, P. Impact of Oat Husk Extracts on Mid-Stage Cement Hydration and the Mechanical Strength of Mortar. *Constr. Mater.* **2024**, *4*, 91–109. <https://doi.org/10.3390/constrmater4010006>

Received: 15 November 2023

Revised: 26 December 2023

Accepted: 9 January 2024

Published: 11 January 2024



Copyright: © 2024 by the authors. Licensee MDPI, Basel, Switzerland. This article is an open access article distributed under the terms and conditions of the Creative Commons Attribution (CC BY) license (<https://creativecommons.org/licenses/by/4.0/>).

1. Introduction

In recent decades, there has been growing concern and awareness about the consequences of climate change and its events due to the continuous impact of human activities on the planet. This has led to the establishment of international agreements and initiatives, such as the Paris Agreement [1] and the European Green Deal [2] initiative, which aim to reduce global warming and tackle climate change by acting in various sectors, including the construction industry.

As part of the European Green Deal and to guide the construction sector, programs such as Renovation Wave [3] and the European Bauhaus [4] initiative were launched to promote more environmentally friendly and energy-efficient construction. These initiatives highlight the significance of resource circularity and using renewable and nature-based materials, such as plant-based resources, to offset carbon emissions and reduce emissions to produce traditional construction materials [3,4].

In light of these recommendations, one strategy adopted by the scientific community was the development of materials focusing on valorising by-products from various production chains, including easily renewable lignocellulosic resources and their uses in composite materials [5–7]. Using lignocellulosic by-product materials is a well-known method for producing wood-based composites, joining particles together using a binder agent. One way to classify composites is based on the binder agent used, such as polymer-bound [8] and mineral-bound composites, and among them cement-bound composites [9].

Currently, studies are exploring the use of forest residues in the production of mineral-based composites, such as hemp hurds [10], for use in lime matrices [11], and the study of different types of wood chips [7,12] and sawdust [13] for use in wood-cement composites.

Considering agricultural by-products, the studies are divided into investigations into residues as fillers or aggregate [14–16], exploring crushed stalks from different crops such as wheat straw [17] and rice straw [18], and the use of husks and hulls as in the case of rice [19] and hazelnut [20], and their use in the form of fibrous reinforcement [7,21], for example, flax [21,22], hemp [21] and jute [23].

One of the potential sources of lignocellulosic resources in Europe comes from the production of oat (*Avena sativa* L.), a member of the *Poaceae* family, which accounts for approximately 60% of the 25.18 million tons produced globally, providing a large volume of husks during the dehulling process that has no well-defined destination, being mostly discarded or buried [24–26]. While abundant across Europe, this resource remains underexplored within the scientific community. Current investigations have primarily focused on exploring its ashes and its potential application as a source of silica [27,28], applied as a bio-modifier in an asphalt binder [29], as well as its utility for cellulose extraction [30] and as a partial substitute in particleboard production [31].

Nevertheless, the adoption of this kind of resource in cement-based matrices faces well-known challenges regarding its compatibility due to the chemical composition variability of lignocellulosic resources. The solubilisation of its surface products, known as extractives, and the products of its degradation in the alkaline environment of lime-based matrices influence both the potential interaction dynamics between the lignocellulosic material and cement phases and the internal interactions intrinsic to the cement matrix, interfering with its hydration and consequently inhibiting its setting and strength development [15,32]. Additionally, as an organic material, oat husks present inherent composition variability. These include relative amounts of lignin, cellulose and ash and can be influenced by genetic type [33] and climate change [34], among other reasons.

Considering the inherent challenges in the production of wood–cement composites [15] and the existing research efforts aimed at facilitating and emphasising the potential use of analogous resources as aggregates in lime-based matrices, such as rice husks [19] and hemp hurds [11,14], there is a compelling opportunity to initiate a research trajectory focused on understanding the interaction between oat husks and lime-based matrices. This begins by gaining comprehensive insights into this material's chemical composition and elucidating the interactive dynamics between its components and the binder [15].

While the presence of lignin has a minor retarding effect on the cement matrix compared to other saccharides, its pure concentration of 1% has been shown to delay cement hydration by more than two days [35]. However, the polysaccharides forming cellulose demonstrate resilience to strong alkaline solutions [10,15], consequently not significantly impeding cement hydration.

Hemicellulose, on the other hand, is a material that dissolves in weak alkaline solutions, releasing low-molecular-weight carbohydrates that can entirely hinder the cement setting process, depending on the concentration [10,15]. In the same way, as noted by Kochova et al. [35], also considering other extractives, more substantial predictive factors for retarding cement hydration lie in the chemical composition and the concentration of leached products.

The development of strength in Ordinary Portland Cement (OPC) is related to the hydration reaction, characterised by processes involving the dissolution and precipitation of anhydrous, soluble aluminates, silicates, and additives that constitute OPC, promoting the solidification of a paste and the densification of its crystalline microstructure. The mineral phases comprising OPC are classified as silicates, namely alite (C_3S) and belite (C_2S), and aluminates, including tricalcium aluminate (C_3A) and calcium aluminoferrite (C_4AF). Additionally, calcium sulphate dihydrate (gypsum) is added to control the velocity of reactions, thereby influencing the workability and setting. As a consequence of the hydration process, matrix solidification occurs, accompanied by the development of strength and the formation of primary reaction products—calcium silicate hydrates (C-S-H) and Portlandite ($Ca(OH)_2$).

The OPC hydration mechanisms are complex processes based on phase transformations that are not yet fully understood. However, from the calorimetric perspective, the phases can be generally classified as follows:

1. Initial period, occurring immediately after contact with water;
2. Induction or dormant period, a period of low reaction rate in which the matrix is still malleable;
3. Acceleration period, which can take hours, characterised by the re-acceleration of reaction rates, consequently solidifying the matrix, with the beginning of this phase corresponding to the initial setting time measured by the Vicat method (this can take hours), but the Vicat's final setting marks a point before its end;
4. And the deceleration period, evidenced by a slowly descending reactivity period of no defined end [36,37].

Due to its complexity, OPC hydration can suffer interference by inhibition mechanisms in any phase, but despite the significant variability among materials, some of the inhibition mechanisms are already known. Among them are the absorption of sugars by cement grains, the precipitation of insoluble components, the complexation of essential ions, the nucleation inhibition of $\text{Ca}(\text{OH})_2$ crystals, and pH matrix changes [38–40]. As ways of mitigating the inhibitory effects of lignocellulosic resources, the strategies employed are mainly divided into pre-treatments for extracting inhibitory components from the material, preventing the release of compounds using particle coating, matrix selection and the use of additives to accelerate the matrix setting [15].

Considering the factors mentioned, this study aims to fill in the lacuna in the current understanding regarding the interaction between the cement matrix and extractives present in oat husks by investigating the medium-term effects of these extractives on cement hydration and exploring strategies for their removal. In this way, the work is committed to chemically characterising the oat husks, assessing the efficiency of various water washing cycles in extractives' removal and investigating the effect of soluble products on cement setting time and the hydration and mechanical strength development under two curing conditions, but limiting the analysis to only between 3 and 28 days.

2. Materials and Methods

2.1. Materials

2.1.1. Binder

Rapid Hardening Portland Cement (RHPC) was chosen in this study because of its minimal secondary addition to emphasising only the interactions between extractives and cement. It was supplied by Irish Cement Ltd. (Platin, Drogheda, Ireland) and classified as CEM-I 42.5 R in compliance with the performance specifications outlined by EN 197-1:2011 Standard [41], according to the producers.

2.1.2. Fine Aggregates

Category 1 natural sand, according to EN 13139:2013 Standard [42], of 0/4 mm particle size range, specific gravity 2.56 g/cm^3 , exhibiting 2.70% fineness modulus and 2.35% fines, was used for the mortar mixing.

2.1.3. Oats Husks

As the lignocellulosic material, the same material as employed in a previous study conducted by Bonifacio and Archbold [27] was utilized. The material consisted of raw oat husks from the Co. Wexford region in the Republic of Ireland, harvested in July 2020. However, the particle size was restricted to only those retained by the 0.5 mm sieve to avoid incorporating extracted oat dust particles.

2.2. Procedures

2.2.1. Binder Chemical Characterization

The phase composition analysis was performed by a scan of anhydrous cement samples in an X-ray diffractometer (PANalytical Aeris, Malvern, UK) using Cu K α radiation (K α 1 = 1.54060 Å | K α 2 = 1.54443 Å | 0.5 ratio) at 40 kV, 7.5 mA through the continuous scan method using fixed divergent slit, PIXcel1D-Medipix3 detector, 0.0220 °2 θ step size and 23.9700 s scan step time from 10.0 to 69.9 °2 θ . The identification and estimate quantification of phases were performed in powder pattern analysis software (Panalytical X-Pert HighScore Plus Version 4.8), and the refinement of the crystalline structures was carried out using the Rietveld method [43] following adjustment procedures suggested by Santos Nobre et al. [44].

2.2.2. Husks' Chemical Characterization

Considering the impact of polysaccharides on cement hydration kinetics, an analysis of the structural component proportions in the cell wall of lignocellulosic materials could provide insights into potential factors hindering cement setting.

The moisture content of the sieved husks was determined by drying four samples, each weighing 5 g, in an aerated laboratory chamber furnace at 60 °C for 42 h. Subsequently, the average percentage difference between the initial mass and the mass after cooling in a desiccator was calculated for each sample. To determine the ash content, six alumina crucibles, each containing 5 g of dried samples, following the above procedure, were calcined in an aerated laboratory chamber furnace at 950 °C for 6 h. The ash content was determined by calculating the average percentage difference between the initial mass and the mass after cooling in a desiccator for each sample using the loss on ignition (LOI) method described by Bonifacio and Archbold [27].

A cartridge containing an excess of 5 g of oat husks was introduced into the Soxhlet extraction system to determine the extractive content. The material underwent approximately 26 reflux cycles (6 h in total) using 150 mL of distilled water as solvent, as toluene/ethanol in a 2:1 ratio and pure ethanol, respectively, were found to be less effective. The determination of total extractives content involved measuring the mass retained in the round bottom flask after solvent evaporation, following drying in an electric oven at 60 °C for 42 h.

The lignin content, which is insoluble in 72% sulfuric acid (Klason lignin), was determined in triplicate, following the TAPPI T 222 om-02 Standard [45]. Nevertheless, adjustments were made to employ unground extractive-free oat husks and filter papers during filtration.

For the holocellulose determination in triplicate, 15 g of moisture-free and extractive-free material was split into three separate Erlenmeyer flasks, each containing 160 mL of distilled water. The flasks were then immersed in a water bath set at 70 °C. An addition cycle commenced with 1.5 g of sodium chlorite (NaClO₂) of approximately 80% purity and 1 mL of glacial acetic acid with purity \geq 99.85%, added per hour until the material achieved complete whitening. Subsequently, the material was allowed to cool for 30 min in an ice bath and then subjected to vacuum filtration using a sintered glass funnel assembled in a Kitassato flask. Filtration continued until the rinsed precipitate reached a neutral pH. The holocellulose percentage was determined by calculating the difference between the initial mass and the mass of the material collected after drying in an oven at 60 °C for 18 h and cooling in a desiccator.

The material obtained during the holocellulose determination was subjected to cellulose content analysis in triplicate. The material was mixed with 100 mL of 5% potassium hydroxide (KOH) solution and allowed to stand at 20 °C for 24 h. Following this period, the material was rinsed until it reached neutral pH, filtered, dried and subjected to cellulose content determination using the same method as for holocellulose. The hemicellulose percentage was calculated as the difference between the final holocellulose and the cellulose content percentages.

2.2.3. Extractives' Removal

Oat husks were dried in an electric furnace at 60 °C for 42 h, and the material retained on the 1 mm mesh sieve was utilised to assess extractive removal. The methods used for 2 and 6 h cycles of extraction in hot water (~100 °C) and 1 h cycles using cold water (23 ± 2 °C) adhered to the ASTM D1110-21 [46], with the sample immersion period, the use of 5 g of unground samples and the use of the blue band qualitative filter paper and funnel instead of the alundum or fritted-glass crucible serving as the sole modifications.

To determine the maximum extractives removed in a single immersion cycle with the longest possible retention time (considering that the highest concentration of saccharides and uronic acid is obtained after 24 h, as noted by Page et al. and Sedan [22,47], 20 g of these husks were placed in a glass container filled with 200 mL of distilled water (0.1 husk/water ratio) at 20 ± 3 °C.

For extraction in an alkaline solution, 20 g of dried husks were immersed in 200 mL of a solution prepared by mixing Ca(OH)₂ and distillate water (1.580 g/L) at 20 ± 2 °C in a glass container.

After 6 and 24 h of immersion, the glass container was drained using a 0.5 mm mesh for both mixtures. Subsequently, after four repetitions, all the containers were dried in an electric oven at 60 °C for 72 h. The percentage of extractives removed was calculated by determining the average percentage difference between the initial sample mass and the mass of the material retained in each container after drying and cooling in a desiccator.

2.2.4. Leached Mixing Water

Mixing water containing extractives was prepared by soaking oat husks in a solution at 20 °C for 24 h, using a 1:10 liquid/mass ratio and filtering them through the 0.25 mm mesh. For the Vicat test only, husks were kept for 6 h in boiling distillate water and immersed for more than 18 h until the water cooled to room temperature (Sample LBW).

Two types of solution were utilised during the extraction: distillate water (Sample CW) and a solution made of Ca(OH)₂ mixed with distillate water at a concentration of 1.580 g/L (Sample CCH), reaching a theoretical pH of 12.63, intended to promote the removal of extractives and the degradation of husks in alkaline environment. The solutions obtained after extraction received the prefix "L", and were named Sample LW and Sample LCH, respectively. The pH of each solution was measured using a pH meter (Model Jenway 3520, Cole-Parmer, Saint Neots, United Kingdom) before immersing the sample and after obtaining the filtered solution.

2.2.5. Mixing Procedure

All mixtures were prepared using an electric hammer drill (Black+Decker 710 W, Leinster, Ireland) controlled by a generic external speed controller and a plaster paddle mixer, replicating the procedure to prepare a standard-consistency cement paste [48]. The mixing process involved combining cement and mixing water in a 5-litre bowl. Initially, the mixer operated at 200 ~ 250 rpm for a 30 s mixing period, followed by a 30 s pause to scrape the paste from the bowl walls. Subsequently, mixing was resumed using 250 ~ 300 rpm for 60 s.

2.2.6. Vicat Testing for Monitoring Cement Setting

The procedure for assessing the cement setting time was executed in triplicate and adhered to the guidelines outlined in the EN 196-3 Standard [48]. A mixture of normal consistency, prepared using 500 g of cement and 130 mL of solution, was mixed according to the procedure mentioned in Section 2.2.5. The solutions used and their preparation consist of those previously indicated in Section 2.2.4, which consisted of control samples (Sample CW and Sample CCH) and solutions containing extracted material (Sample LW, Sample LBW and Sample LCH).

This mixture was then poured into a truncated cone-shaped mould 40 mm deep, as per the standard. The setting time evaluation was performed using an Automatic Vicat testing instrument (Controls Vicamatic 3 63-L2701, Hertfordshire, UK), which involved the

free fall and penetration, at known intervals, of a 300 g set comprising a needle fixed to a moving part. The initial setting was determined when the needle penetrated only 37 mm into the specimen, while the final setting was defined when the needle penetrated only 0.5 mm into the inverted specimen.

2.2.7. Analysis of the Direct Contact between the Sample and the Matrix

To investigate the cement hydration at the interface between the matrix and oat husks, following the approach outlined by Diquélou et al. [11] when examining hemp shivs, a cylindrical tablet of 100 mm diameter and 40 mm thickness prepared by filling a 10 mm evacuable pellet die (Specac) with oat husks and compressing it for 2 min under 8 tons using a manual hydraulic press (15 Ton Atlas-Specac). The tablet was centred at the bottom of a transparent plastic Petri dish. Subsequently, the void space in the dish was filled using a paste made of 200 g cement and 100 g distilled water. The setup underwent a curing process at ~ 21 °C and $>80\%$ humidity using an improvised water mist chamber and generic ultrasonic humidifier.

Following the 28-day curing period, the bottom of the dish was scanned using a conventional scanner at 800 DPI resolution, using a black background (cover open). Subsequently, the obtained image underwent analysis utilising specialised software (ImageJ Version 1.54f Java). Additionally, two samples were collected from the matrix—one from the peripheral region of the tablet (Region 1) and another from a region distant from the tablet (Region 2), according to Figure 1. Both samples were immersed in liquid nitrogen for 20 min and then subjected to freeze-drying at -40 °C for 24 h using a freeze dryer (Heto PowerDry Lyolab 3000) and vacuum pump (ThermoSavant model RV3 A65213906). After the freeze-drying process, the samples were finely ground using a mortar and pestle and subsequently analysed.

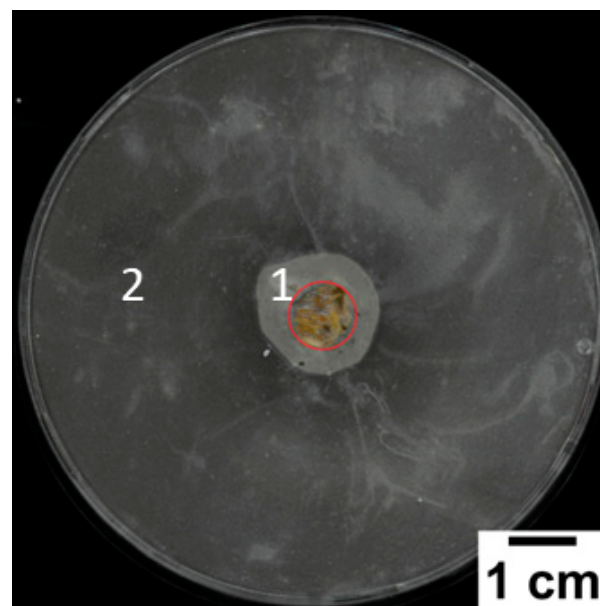


Figure 1. Cement matrix with an oat husk tablet in the centre, with a red projection of the tablet limits and numbers representing the regions from which samples were extracted.

2.2.8. Hydration Analysis

Following the methodology proposed by Diquélou et al. [11] and utilising the mixing procedure outlined in Section 2.2.5, a mixture consisting of 300 g of cement and 150 mL from one of the solutions presented in Section 2.2.4 was prepared. Subsequently, the mixture was poured into six 2 mL plastic microcentrifuge tubes, and each set (six samples) received the same name as the solution used. The process was systematically repeated until one set of samples was obtained for each of the four existing solutions.

Subsequently, one sample for each type of solution used was subjected to immersion in liquid nitrogen for 20 min and freeze-dried at $-40\text{ }^{\circ}\text{C}$ for 24 h at different time intervals (7 days and 28 days after the cement and solution mixing), resulting in a total of 6 samples. Following the aforementioned freeze-drying process, the samples were finely ground using a mortar and pestle and then submitted for thermal gravimetric analysis (TGA) and Fourier transform infrared spectroscopy (FT-IR) analyses.

Approximately 12 mg of each one of the ground samples was used in the thermal gravimetric analysis measurement, carried out in an alumina crucible heated from $30\text{ }^{\circ}\text{C}$ to $940\text{ }^{\circ}\text{C}$ at $10\text{ }^{\circ}\text{C}/\text{min}$ under a $20.0\text{ mL}/\text{min}$ nitrogen flow in a thermogravimetric analyser (Pyris 1 TGA Thermogravimetric Analyzer). The data analysis was performed using specialised software (Pyris Software version 10); the mass loss before $120\text{ }^{\circ}\text{C}$ was discarded to avoid free water influence, and the range from $120\text{ }^{\circ}\text{C}$ to $350\text{ }^{\circ}\text{C}$ was considered to be the dehydration of hydrates (LDH), including C-S-H; the range between 350 ° and $550\text{ }^{\circ}\text{C}$ was considered to be indicative of the dehydroxylation of Portlandite (LDX), and between $550\text{ }^{\circ}\text{C}$ and $940\text{ }^{\circ}\text{C}$ (LDC) as the decarbonation of calcium carbonate (CaCO_3) indicative [49,50]. The percentage of hydrates, Portlandite and CaCO_3 can be quantified by applying Equations (1)–(3), respectively [11], in which the mass loss observed for each range is multiplied by the quotient of the molar mass of Portlandite (74), pure water (18.01528), CaCO_3 (100.0869) and carbon dioxide (44.01).

$$\text{Bound Water (\%)} = \text{LDH (\%)} \quad (1)$$

$$\text{Portlandite (\%)} = \text{LDX (\%)} \times (74/18.01528) \quad (2)$$

$$\text{CaCO}_3 (\%) = \text{LDC (\%)} \times (100.0869/44.01) \quad (3)$$

Fourier transform infrared spectroscopy analyses were conducted at room temperature using an infrared spectrometer (PerkinElmer Spectrum One) equipped with a universal attenuated total reflection (ATR) sampling accessory, applying a consistent fixed universal compression force of 85 N. Each sample underwent four scans in the spectral range examined, from 650 to 4000 cm^{-1} .

2.2.9. Mechanical Tests

Using the mixing procedure presented in Section 2.2.5, mortars were prepared by combining 1350 g of cement, 4050 g of sand and 675 mL of one of the solutions presented in Section 2.2.4. Subsequently, the mortar was transferred to three sets of three prisms, each measuring $40 \times 40 \times 160\text{ mm}$, following the specifications outlined in the EN 196-1 [51] Standard, forming 2 cm thick layers with each layer vibrated for 5 s on a vibrating table. The process was repeated, and the samples were given names corresponding to the solution used, among those listed in Section 2.2.4.

The mortars were left to cure for 24 h under 50% humidity and $21\text{ }^{\circ}\text{C}$ until demolding. The entire procedure was repeated, configuring a set of nine samples curing under $\sim 50\%$ humidity (positioned over the water) and $\sim 21\text{ }^{\circ}\text{C}$ environment (Sample name—A), and another set immersed in water at $21\text{ }^{\circ}\text{C}$ (Sample name—B). Both sets were kept curing until the test ages (3, 7, and 28 days) and were submitted to specific density evaluation using an industrial specific gravity balance (Stable Micro Systems SG/15-395).

The flexural and compression tests were conducted in accordance with EN 196-1 Standard [51] guidelines, employing a universal testing machine of capacity 300 kN (Instron 300DX-B1-G4-G1A, INSTRON, Norwood, MA, USA) for the flexural test and the 2000 kN capacity compression machine (ELE ADR Touch SOLO 2000, ELE International, Leighton Buzzard, UK) for the compression test.

2.2.10. Statistical Analysis and Chart Production

The statistical analyses were performed using built-in programs in statistical software (Minitab Version 20.3) that calculated the mean and standard deviation (S.D), checked for outliers and calculated the confidence interval (C.I), implementing the two-tailed Student's

T-distribution with a 95% confidence level and degrees of freedom equal to the number of samples minus one. According to criteria adapted from observations made by the American Concrete Institute [52] for the overall variation of laboratory trial batches, samples with S.D values less than 5 were accepted as valid results for mechanical tests. All charts were produced using interactive scientific graphing software (OriginPro Version 2023).

3. Results and Discussions

3.1. Binder Mineral Phases Composition

The potential phases and concentration of the cement utilised are summarised in Table 1. The statistical indices for the analysis of the diffractogram calculated by the software used present values for assessing data noise using the Rexpected index (Rexp) equal to 5.23, with lower values indicating greater quality. Weighted adjustment indices of the residual difference between observed and calculated plots, known as weighted profile R-factor (Rwp), had a value of 4.01 and goodness of fit (Gof) was 0.58, where indices less than 4 indicate good fit, coming from the quotient of the two preceding indices squared.

Table 1. Cement CEM I 42.5 R possible mineral phase composition.

Mineral Phase	Cement Chemist Notation	(%)	Chemical Formula	ICSD Code
Alite	C ₃ S(monoclinic)	58.0	Ca ₃ SiO ₅ -Mg, Al	94742
Belite	C ₂ S(monoclinic)	17.2	Ca ₂ SiO ₄	81096
Aluminate	C ₃ A(cubic)	4.6	Ca ₃ Al ₂ O ₆	1841
Aluminate	C ₃ A(orthorhombic)	0.1	Ca _{8.5} NaAl ₆ O ₁₈	100220
Ferrite	C ₄ AF	9.2	Ca ₂ AlFeO ₅	9197
Gypsum	C \bar{S} H ₂	2.4	CaSO ₄ .2H ₂ O	151692
Anhydrite	C \bar{S}	2.3	CaSO ₄	24473
Hemihydrate	C \bar{S} H _{0.5}	0.5	CaSO ₄ .0.5H ₂ O	79528
Portlandite	CH	2.8	Ca(OH) ₂	15471
Calcite	C \bar{C}	2.9	CaCO ₃	80869

Assuming the material is in accordance with the specifications outlined by EN 197-1:2011 Standard [41], we consider the values presented only as approximate indications of the identified phases since, according to Toby [53], despite lower values for profile fitting are frequently presented as indicative of a better quality of the analysis carried out, the indices are subject to several discrepancies, requiring the execution of more complex and detailed analyses, which go beyond the scope of this study, to obtain more precise results.

3.2. Oat Husk Composition and Removal of Extractives

The examination of oat husk composition, as detailed in Table 2, highlights the high lignocellulosic content, constituting 91.19% of the total dried husks' mass.

Table 2. Chemical composition of oats husks based on sample dry weight compared to data adapted from Neitzel et al. [54] and also adapted from Schmitz et al. [34].

Components	(% of Dry Weight Mass)	C.I (95%)	Adapted from Neitzel et al. [54] (%)	Adapted from Schmitz et al. [34] (%)
Lignin (Acid Soluble)	20.28	±0.47	25.44	25.40
Holocellulose	70.90	±1.96	66.19	50.30
Cellulose	33.65	±2.07	29.80	17.20
Hemicellulose	37.25		36.39	33.10
Soxhlet extractives (Water as solvent)	5.01	±0.26	16.98 b	
Ash	1.99 c	±0.01	6.27 b	6.00 b
Others	1.81	±0.00	2.10 a	18.30 a

(a) Include extractives and other substances; (b) not Soxhlet and carried out in an analysis separate from the composition analysis; (c) analysis carried out separately using 950 °C as final temperature.

As the primary composition consisted of holocellulose, making up about two-thirds of the dry mass, and with hemicellulose accounting for approximately 52.56% of this

fraction, further consideration is warranted. Moreover, considering the material was neither ground nor cleaned before analysis, the reported percentages of extractives, ashes and other components may overlap due to hot water reflux that carries away water-soluble constituents and other elements found in the pores and surface of the oat husks, including dust and chemical elements outlined in Table 3.

Table 3. Chemical elements identified on the surface of oat husks, according to data adapted from Bonifacio and Archbold [27].

Component	C	O	Al	Si	K	Ca
Weight husk (%)	35.21	59.65	0.59	3.47	0.97	0.11
Weight ash (%)	0	46.94	0.64	23.84	15.17	4.79

The lignocellulosic percentage is similar to results observed by other authors. However, similarly to results observed by Neitzel et al. [54], the cellulose percentage is lower than lignin, differing from the results observed by Schmitz et al. [34], who argued that oat hulls typically have a higher percentage of lignin in relation to cellulose.

High percentages of cellulose contribute by competition to the natural reduction of other components with a more significant potential for dissolution in alkaline environments and for delaying or interfering with the hydration process, considering that cellulose does not significantly influence the process [10,15]. However, lignin [35] and hemicellulose [10,15] can retard or entirely hinder the cement setting process by dissolving in weak alkaline solutions.

The relatively low ash proportion, even when comparing results observed by other authors, suggests a minor mineral content compared to the lignocellulosic fraction. However, an elemental analysis of these ashes, presented in Table 3, reveals a notable presence of silicon (Si), followed by potassium (K), compared to other elements. According to Bonifacio and Archbold [27], this ash content variation can be attributed to calcination conditions, such as oxygen availability, exposure time, temperature, heating ramp and the presence of elements like potassium. Specifically, the presence of potassium oxide observed by the authors can promote the formation of a surface film, confining the carbon and preventing its volatilisation [55].

Oat Husks and the Removal of Extractives

The immersion of oat husks in hot water (~100 °C) for 6 h led to the removal of 5.34% more than the total extractives removed during 24 h immersion in cold water (23 ± 2 °C), also presenting higher percentages after 2 h immersion, as shown in Table 4, obtained during Soxhlet extraction using hot water reflux. When considering the gradual removal of extractives, conducting washing cycles using cold water pointed to a gradual reduction in extractives responsible for the colour, as seen in Figure 2, in addition to the decrease in the material’s characteristic odour immediately after the second wash.

Table 4. Extractive removal summary by number of washing cycles and immersion time.

Washing Cycles	Duration	Extraction Method	Extractives Removed (%)	C.I (95%)	Number of Samples	S.D
1	2 h	Hot Water	8.702	±0.349	5	0.281
1	6 h	Hot Water	16.266	±0.353	5	0.285
1	12 h	Cold Water	13.385	±0.179	5	0.144
1	24 h	Cold Water	15.441	±0.107	5	0.086
1	6 h	Ca(OH) ₂	9.517	±0.961	4	0.774
1	24 h	Ca(OH) ₂	27.345	±0.519	5	0.326
1	1 h	Cold Water	1.362	±0.537	4	0.338
2	1 h	Cold Water	0.275	±0.080	4	0.050
3	1 h	Cold Water	0.162	±0.076	4	0.048
4	1 h	Cold Water	0.150	±0.113	4	0.071
5	1 h	Cold Water	0.083	±0.313	3	0.126
Σ _{{i = 1}^5} i		Cold Water	2.033			

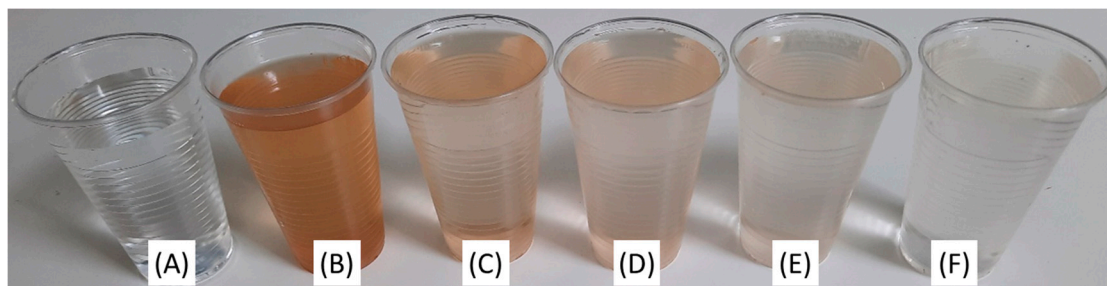


Figure 2. Indicating (A) the control solution made from pure water, and the solutions after 1 washing cycle using cold water (B), 2 cycles (C), 3 cycles (D), 4 cycles (E) and 5 cycles (F).

Numerically, there was a 13.41% difference in material removed using cold water after a single 24 h cycle over five 1-h cycles, representing 7.59 times more efficiency. The 1 h cycles together removed approximately 2.03% of the material mass, within which the first cycle (1 cycle) removed about 67% of these the extractives and surface products (67%). Subsequent cycles removed materials at considerably reduced rates.

Results obtained regarding hot or cold water use were similar to those observed by other authors, who indicated a more significant amount of extractives when using hot water than in tests using cold water [54,56]. The method used might have contributed to some of the difference between hot water extraction and Soxhlet extraction, as one is based on the mass of material accumulated in the solution bottle after drying, which is sensitive to particle retention by the filter, and the other on the mass of material lost by the sample. Extraction with $\text{Ca}(\text{OH})_2$ showed a more significant removal of extractives than other methods, although corresponding to a lower mass reduction than the effect of exposure during the same time interval to a solution made of a strong base, such as the potassium hydroxide (KOH), used to remove hemicellulose during the chemical characterisation process.

3.3. Extractives' Influence on Cement Setting Time and Solutions' pH

The pH measurements performed during the preparation of all solutions revealed, as shown in Table 5, that extractives exhibit an acidic character, as evidenced by the reduction in pH. In terms of setting, results presented in Table 6 indicate a longer setting time in samples containing extractives, in which cold water extractives caused a 31.74% overall delay and hot water extractives caused a 52.40% delay relative to the control specimen (Sample CW).

Table 5. Summary of the pH of solutions at the beginning and end of preparation.

Measurement	Sample CW	Sample CCH	Sample LW	Sample LCH
Initial pH	6.532	12.855	6.954	12.855
Final pH	6.421	12.741	5.652	10.245

Table 6. Vicat test start and end times using different mixing water.

Formulation	Initial Setting Time (Hour:Minute:Second)	C.I (95%)	Final Setting Time (Hour:Minute:Second)	C.I (95%)
Distilled water (Sample CW)	02:19:02	±00:14:21	02:36:59	±00:18:18
Cold-water leached (Sample LW)	02:39:21	±00:19:03	03:26:48	±00:10:32
Hot-water leached (Sample LBCW)	02:50:55	±00:16:53	03:59:14	±00:22:54
$\text{Ca}(\text{OH})_2$ solution (Sample CCH)	02:24:04	±00:01:00	03:19:04	±00:08:04
$\text{Ca}(\text{OH})_2$ leached (Sample LCH)	03:02:03	±00:05:26	04:32:03	±00:03:02

When considering the hydration stages, the delay in the induction stage increased by 14.62% when using cold water extractives, compared to a 22.93% increase when using hot water extractives, representing an 8.31% difference between the two. On the other hand, to reach the final Vicat's setting time, part of the hydration's acceleration stage, cold water extractives, caused 164.35% delay, which is 116.31% less than that caused by using hot water extractives, resulting in 280.66% delay.

The induction stage and final setting time when using Sample CCH increased by 3.5% and 21.1%, respectively, compared to Sample CW. Furthermore, there was a 20.9% and 26.8% difference in the Sample CCH for the same stages when it contained extractives.

It is known that pH variation impacts the solubility and stability of hydration elements, promoting detrimental effects on strength development [57]; for this reason, associated with the presence of saccharides, it may be one of the inhibition mechanisms acting to reduce the reaction rate. Furthermore, the extended setting interval and strength development delay may indicate interference in the hydration product development, which is well known when in the presence of components that act as nucleation/surface adsorption poisoners and favour chelating mechanisms [58].

Based on the setting delay and the fact that the mass of oat husks used to prepare the solutions only makes up 2.6% of the total cement used, the findings may be considered significant if assuming, in basic terms, that each gram of oat husks utilised caused the overall delay of 2.44% and 4.03% for cold and hot water extractives, respectively.

3.4. Impact of Extractives on Hydration Product Formation

3.4.1. Identification of Functional Groups in the Presence of Extractive Solutions

The setting time delay indicates changes in the mechanism or the hydration progress. Alterations in the formation of hydration products can be observed through the analysis of FT-IR spectra of samples after 3 days of hydration in Figure 3 by the absence or lower intensity of some characteristic functional groups compared to the control samples.

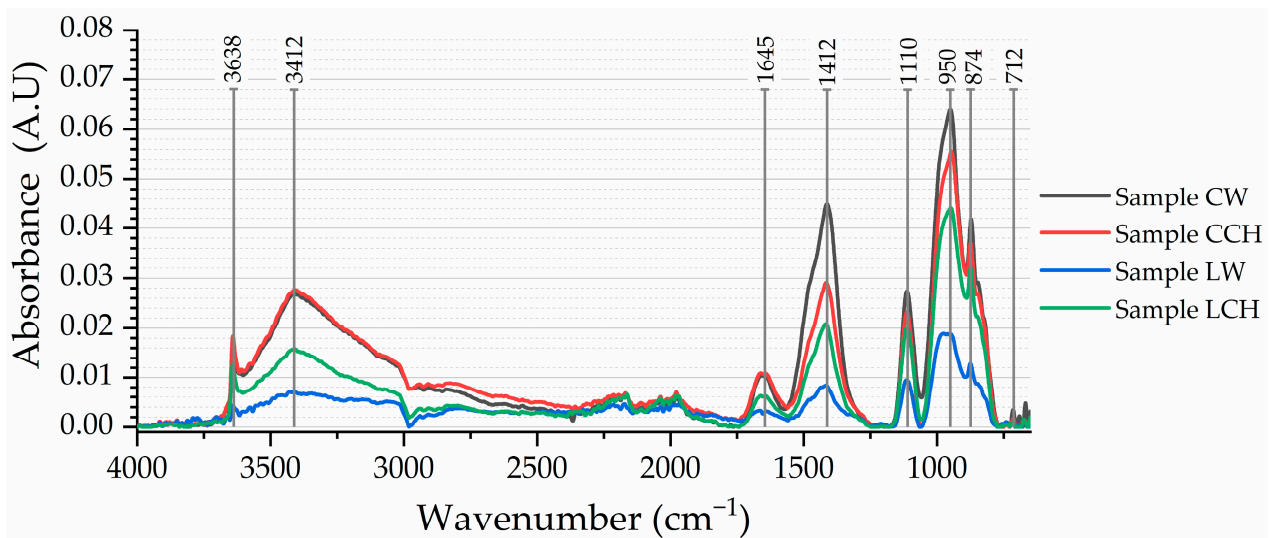


Figure 3. FT-IR spectra of cement samples after 3 days of hydration.

The samples containing extractives presented lower-intensity absorbance peaks at 3638 cm^{-1} , indicative of $\text{Ca}(\text{OH})_2$, present as a hydration product of silicate phases during the cement hydration [59,60]. It is also possible to visualise a significant difference in peaks at 3412 cm^{-1} , which may correspond to the vibration of functional groups in adsorbed water molecules, and specifically O-H stretching vibrations (ν_1 and ν_3) [59,60].

In the lower wavenumber region, it is possible to identify divergences in adsorbed water band peaks located at 1645 cm^{-1} of the four spectra, related to the bending vibration (ν_2) of the H-O-H groups [60], and also some sharp and broad peaks at 1412 , 874 and 712 cm^{-1} , linked to anhydrous CaCO_3 present as a filler or carbonated calcium hydroxide [61].

Some weak peaks are also visible at 1110 cm^{-1} , corresponding to SO_4^{2-} vibration (ν_3) in sulphates, and also in the region of 950 cm^{-1} , which lowers intensity when extractives are added and may be related to the polymerisation of SiO_4 and the formation of C-S-H, generally associated at 960 cm^{-1} , that tends to shift position to a higher wavelength the greater the degree of polymerisation [59,61].

Especially when examining the peak associated with C-S-H formation within the 970 to 920 cm^{-1} range, Sample LW demonstrated the lowest absorbance, evidencing that the samples employing leached solutions exhibited a reduced absorbance compared to Sample CW. If validated by additional experimental techniques applied to quantifying cement hydration products, this observation may indicate the level of inhibition resulting from extractives removed during the extraction process.

3.4.2. Analysis of the Thermal Degradation of Cement Hydration Products

The thermogravimetric assessment results for the decomposition of chemically bonded water and hydration products, such as Portlandite and its carbonated form, CaCO_3 , indicate an increase in bound water content within the 25-day interval for all samples except Sample CW (-0.24%), as shown in Figure 4. Notably, there was a 0.91% increase in Sample LCH. Considering that the bound water temperature range corresponds to some products of the final hydration (C-S-H), but also intermediate phases (as Ettringite) [62], when considering the use of components with the potential to influence the velocity and mechanisms of reactions, the results are significant only when associated with the observation of other products.

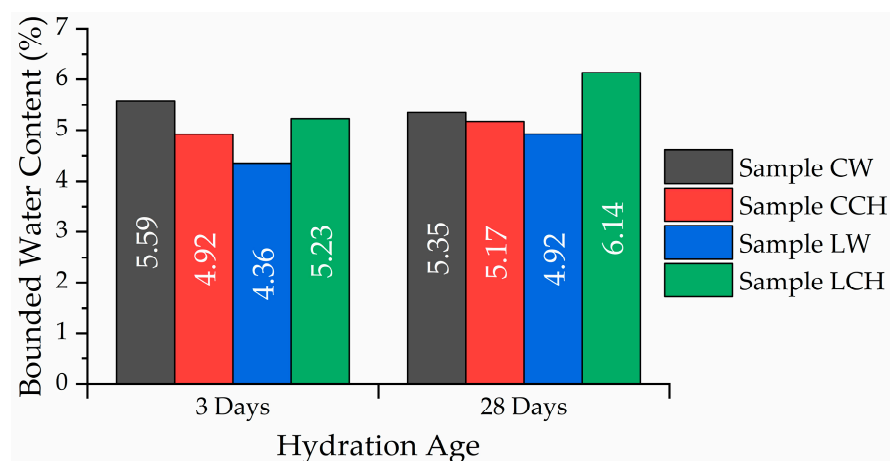


Figure 4. Percentages of chemically bonded water present in each sample as a function of hydration time.

The results also indicate lower portlandite content in samples made using extractives compared to the control samples, as observed in Figure 5. Additionally, it is evident that after 25 days, Sample CW exhibited a decrease in the percentage of Portlandite, in contrast to Sample CCH and Sample LCH, which showed a percentage increase. However, as presented in Figure 6, concerning the presence of CaCO_3 there was only a percentage increase in Sample CW ($+2.55\%$) and Sample LW ($+1.10\%$).

Considering that Portlandite is one of the products generated during the formation of C-S-H during cement hydration, the percentage increase indicates the reaction development. However, the formation of CaCO_3 derived from a possible carbonation of Portlandite must be evaluated. Considering this, the findings suggest an excess of CaCO_3 , more significant than the possible carbonated Portlandite, totalling 1.43% for Sample CW, 0.38% for Sample CCH, 1.33% for Sample LW and 1.06% for Sample LCH.

The appearance of excessive CaCO_3 may be related to the interaction between Portlandite and carbon dioxide (CO_2) from the atmosphere, from the hydration products observed, from the composition of the cement used, as presented in Table 1, or due to pre-

vious hydration promoted by early contact with moisture and the consequent carbonation of the OPC components.

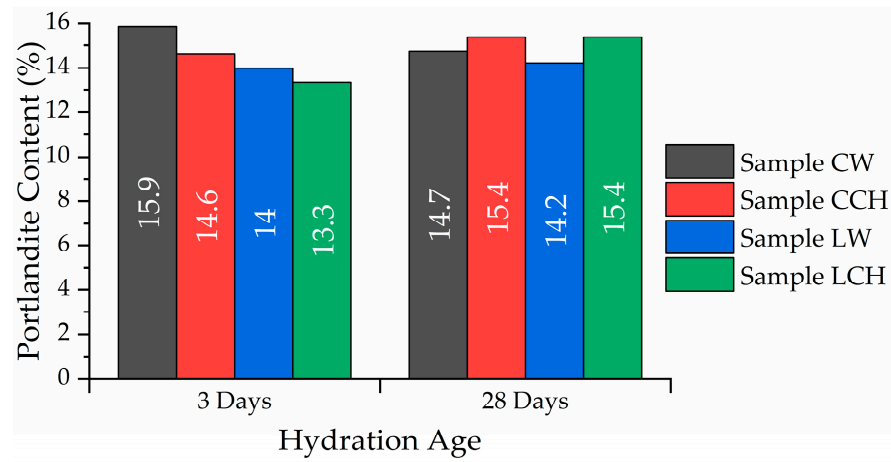


Figure 5. Percentage of Portlandite present in each sample as a function of hydration time.

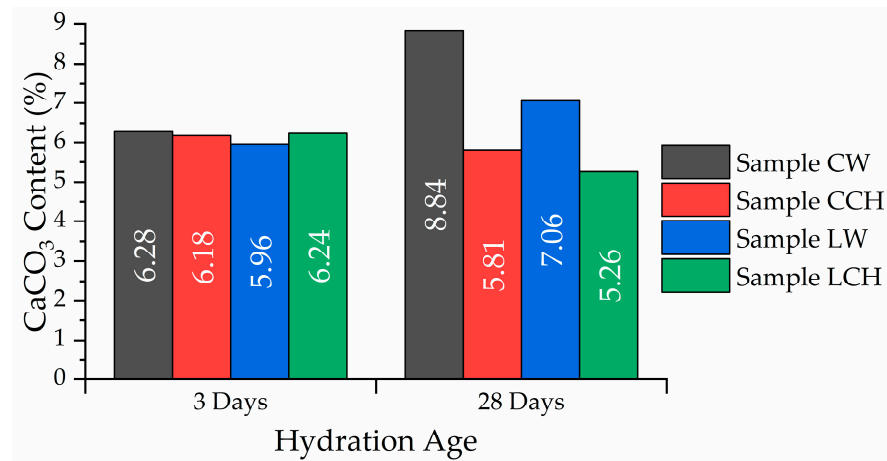


Figure 6. Percentage of CaCO₃ present in each sample as a function of hydration time.

In general, the summed values observed for Portlandite and CaCO₃ in the samples after 3 and 28 days represent, respectively, 22.14% and 23.57% for CW, 20.81% and 21.19% for CCH, 19.95% and 21.28% for LW and 19.58% and 20.64% for LCH.

The presence of compounds capable of modifying the velocity of hydration reactions can be noted by observing that after 3 days, samples without extractives (Sample CW and Sample CCH) showed superior results. However, with the progressive development of the reactions, all samples (Sample CCH, LW and LCH) reached similar values at 28 days but were still lower than those observed in Sample CW at 3 days.

It is supposed that the additional particles present in the mixture act as nucleation/surface adsorption poisoners and favour the chelating mechanism [58], which may also be associated with a reduction in the mobility of the compounds since it is not possible to differentiate the partial or non-hydrated material that could be trapped and present different hydration ages.

The late reaction of cement components due to the change in the reaction velocity by the mechanisms described previously may be one of the justifications for the difference in the overall mass loss over the 25-day interval after excluding free water, representing 1.89% for Sample LW and 1.97% for Sample LCH, compared to 1.19% for Sample CW and 0.64% for Sample CCH.

The interference of oat husk components in the hydration process becomes evident when, as shown in Figure 1, when looking at the effects of direct husk contact with the

matrix after 28 days of hydration, a light-coloured halo of 4.22 mm thickness from the edge of the husk tablet can be seen. Additionally, the thermogravimetric examination presented in Figure 7 reveals differences between the two locations examined, totalling the combined difference of 10.09% in CaCO₃, 83.26% in Portlandite concentration and 86.52% in bound water related to C-S-H formation. The leaching of extractives and degradation compounds from the husks into the matrix may have caused these variations, which point to changes in cement hydration.

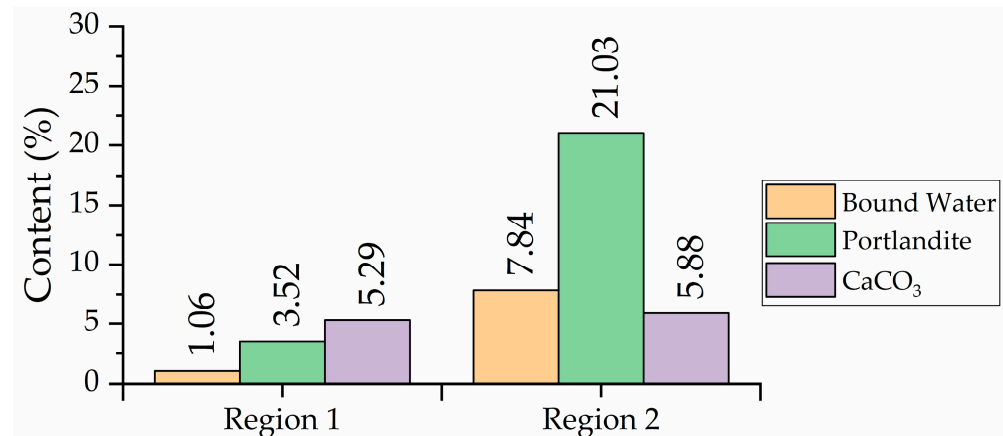


Figure 7. Percentage of each hydrate found in samples extracted from each region after 28 days of hydration.

A halo formation in the transition region, as observed by Diquélou et al. [11] when testing hemp shivs after 3 days of hydration, indicates non-hydrated cement. This is evidenced by the absence of C-S-H and Ca(OH)₂ peaks observed by the authors in FTIR analysis, aligning with the low quantity of hydration products observed in the TGA analysis in the present study.

3.5. Influence of Extractives on Mechanical Properties

When considering the macrostructure development, as observed in Figure 8, both Sample CW and Sample CCH exhibited overall specific densities of 93.1% at 3 days and 96% at 7 days, respectively, relative to the density observed at 28 days. When comparing Group A and Group B, the analysis revealed that Group B exhibited an average difference of 16% for Sample CW, 10% for Sample CCH, 0.4% for Sample LW and 0.1% for Sample LCH compared to Group A. Conversely, when observing individual groups, Group A demonstrated an average difference of 5.79% for Sample CCH, -8.5% for Sample LW and -7.9% for Sample LCH in contrast to Sample CW. Furthermore, comparing Sample CW, Group B demonstrated an average difference of -0.2% for Sample LW, -6.49% for Sample LCH and -6.79% for Sample LCH.

Upon analysis, only approximately 7% of the total volume was attained after the first 3-day hydration period. The samples containing extractives (LW and LCH) developed lower densities than the control groups (CW and CCH) and, unlike these, did not show significantly favourable effects on density gain when increasing water availability through water immersion.

Regarding flexural strength, as depicted in Figure 9, averages of 73.9% and 87.3% of the 28-day results were observed at 3 and 7 days, respectively. Compared to Group A, Group B exhibited average differences of 2% for Sample CW, 5% for Sample CCH, 8% for Sample LW and 20% for Sample LCH. Additionally, Group A displayed an average difference of 3.98% for Sample CCH, -2.55% for Sample LW and -20.17% for Sample LCH. In contrast to Sample CW, Group B exhibited an average difference of 8.24% for Sample CCH, -7.70% for Sample LW and -4.73% for Sample LCH.

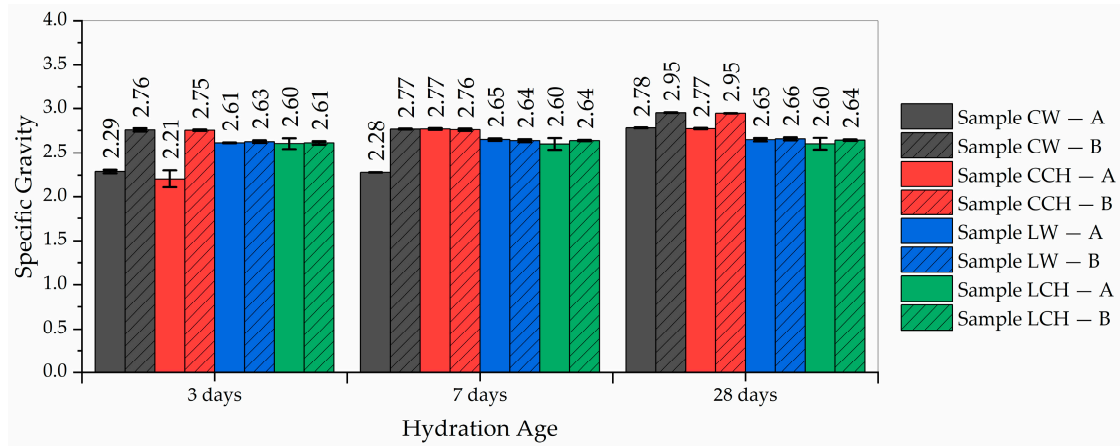


Figure 8. Specific gravity for each sample type as a function of hydration time with standard deviations indicated by error bars.

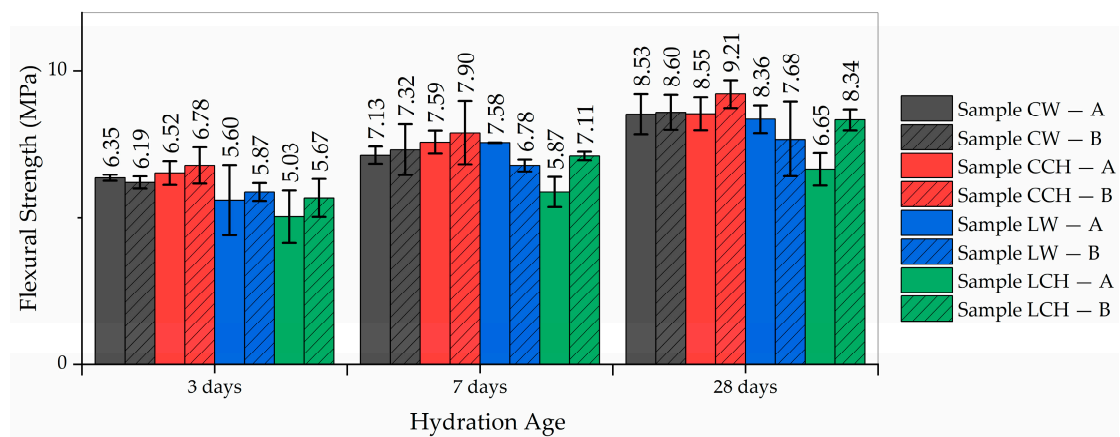


Figure 9. Average flexural strength for each sample type as a function of hydration time with standard deviations indicated by error bars.

The results indicated that approximately 26% of flexural strength developed within 25 days, and flexural strength development was favoured by immersing the samples in water, especially in samples containing extractives (LW and LCH).

Regarding compressive strength performance, as illustrated in Figure 10, 59.7% and 82.1% of the 28-day overall results were observed at 3 and 7 days, respectively. When comparing Group A to Group B, notable differences emerged; Group B exhibited an average difference of 9% for Sample CW, 11% for Sample CCH, 5% for Sample LW and 48% for Sample LCH. Additionally, Group A displayed an average difference of 1.4% with Sample CCH, -9.41% with Sample LW and -36.4% with Sample LCH. In contrast, compared to Sample CW, Group B exhibited an average difference of 3.24% for Sample CCH, -19.50% for Sample LW and -13.71% for Sample LCH.

It is possible to observe that the initial 3-day interval after cement hydration contributes to the compressive strength development more than the approximately 40% of strength developed in the subsequent 25-day interval. In general, samples containing extractives (LW and LCH) developed less compressive strength than control samples (CW and CCH). However, excluding LW, all benefited from immersion in water, in which samples containing or exposed to portlandite (CCH and LCH) showed a significant gain in strength compared to non-immersed samples (CW and LW). In general, an increase of approximately 3.71% in flexural strength and 5.71% in compressive strength per percentage increase in volume was observed within 25 days.

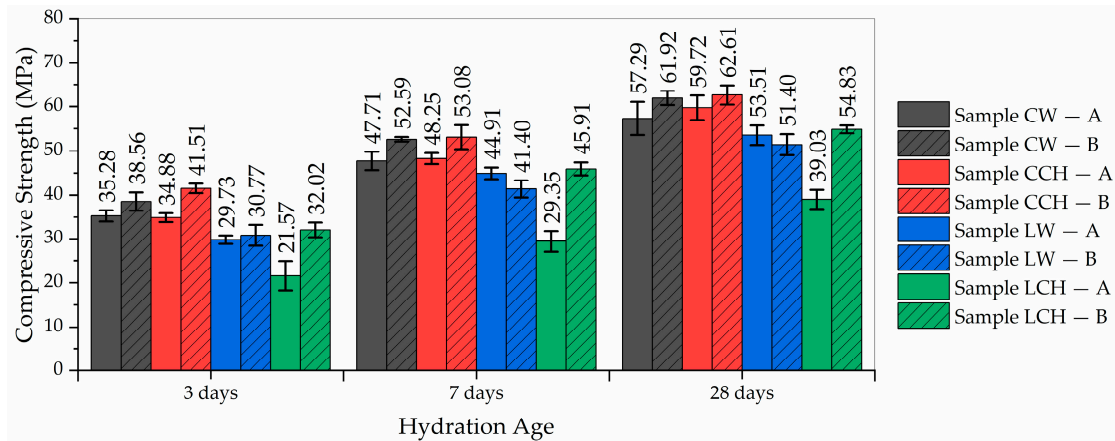


Figure 10. Average compressive strength for each sample type as a function of hydration time with standard deviations indicated by error bars.

Considering that there is a moderate to strong positive correlation between the density and flexural strength (0.578 Pearson, 0.711 Spearman) and compressive strength (0.657 Pearson, 0.829 Spearman) of Sample CW, despite developing higher densities, samples containing extractives showed a reduction in mechanical performance in the range of 8% to 32% in compressive terms and 2% to 21% in flexural terms, which indicates failures in the development of hydration mechanisms and microstructure development or composition.

The increase in the mechanical performance of samples immersed in water is already known [63]. However, in addition to the thermal stability needed for the reactions to occur, this improvement may be related to the better hydration of the innermost regions of the samples due to the greater or longer supply of water to the development of reactions and ion mobility, promoting more significant densification and organisation of the microstructure.

The microstructure densification and leaching of $\text{Ca}(\text{OH})_2$ from samples [64] may be among the reasons for the lower densities observed in Sample CW at 3 and 7 days, hindering the penetration of water into deep regions by blocking pores, thereby affecting the density assessment conducted through the applied methodology.

A similar hypothesis can explain the slight variation in density but lower development of strength in samples containing extractives, in which the inhibitory components present in the extractives prevent or delay the hydration of central regions, while the densification of the sample occurs in the superficial regions due to the interaction of these agents with external humidity.

The strength increase observed in LCH when immersed in water may be another indication of inhibitory agent dissolution, contributing to an improvement in the mechanical behaviour of samples exposed to $\text{Ca}(\text{OH})_2$. This observation can also be associated with the idea that the addition of small amounts of $\text{Ca}(\text{OH})_2$ is favourable for reducing the reaction delay and increasing the availability of nucleation sites [37].

When considering the concentration of inhibitory agents and samples not cured in water, preventing the possible dissolution of inhibitory components, Sample LCH, unlike Sample CCH, which showed an improvement in mechanical performance, indicates lower results, pointing to the existence or greater concentration of inhibitory substances, possibly from the degradation of husks in an alkaline environment [10,15], in line with the results obtained in the analysis of hydration products at the interface between the matrix and the tablet made of oat husks.

4. Conclusions

This study provided a better understanding of the medium-term effects of interactions between cementitious matrices and oat husk constituents, with particular emphasis on extractives. These extractives were found to delay and limit the setting and strength development of the cementitious matrix, indicating a more pronounced limiting effect in

the presence of products resulting from oat husk degradation. The study also allows for the extrapolation of several additional conclusions, namely:

- The examined oat husks exhibited high lignocellulosic content, primarily holocellulosic cellulose content, greater than lignin;
- Hot water proved to be more effective than cold water in removing extractives;
- The duration of immersion is more relevant than the number of washing cycles for the effective removal of extractives;
- Cold water extractives resulted in a setting delay of 2.44% per gram of cement, while hot water extractives caused a delay of 4.03% per gram of cement;
- The presence of extractives significantly influences the duration to reaching the final setting of the matrix.

The insights derived from this research are crucial for guiding treatment strategies to improve the compatibility of oat husks and cementitious matrices, including methods to prevent degradation at early stages and extractive removal. Expanding on the limits of this work for a deeper understanding of the inhibition mechanism associated with the use of this material, complementary studies involving evaluating the composition of the extractives and investigating hydration at early stages using analytical techniques such as calorimetry, TGA, XRD and scanning electron microscopy are suggested.

Author Contributions: Conceptualization, A.L.B.; methodology, A.L.B.; formal analysis, A.L.B.; investigation, A.L.B.; resources, A.L.B. and P.A.; data curation, A.L.B.; writing—original draft preparation, A.L.B.; writing—review and editing, A.L.B. and P.A.; visualization, A.L.B.; supervision, P.A.; project administration, A.L.B.; funding acquisition, P.A. All authors have read and agreed to the published version of the manuscript.

Funding: This research was funded by the Technological University of the Shannon: Midlands President Doctoral Scholarship fund [PA21467].

Data Availability Statement: Data are available on request due to restrictions of privacy.

Acknowledgments: The authors would like to personally express their gratitude to Gilberto Nunes Bezerra for his overall support and to Tielidy Angelina de Moraes de Lima for her invaluable laboratory assistance and contributions to the thermogravimetric analyses.

Conflicts of Interest: The authors declare no conflicts of interest.

References

1. Horowitz, C.A. Paris Agreement. *Int. Leg. Mater.* **2016**, *55*, 740–755. [CrossRef]
2. European Commission. Communication from the Commission to the European Parliament, the Council, the European Economic and Social Committee and the Committee of the Regions. The European Green Deal. Brussels. 2019. Available online: https://cor.europa.eu/en/events/Documents/COTER/ec_communication_eu_missions.pdf (accessed on 30 October 2023).
3. European Commission. A Renovation Wave for Europe—Greening Our Buildings, Creating Jobs, Improving Lives. Brussels. 2020. Available online: <https://eur-lex.europa.eu/legal-content/EN/TXT/?uri=CELEX:52020DC0662> (accessed on 30 October 2023).
4. European Parliament. European Parliament Resolution of 14 September 2022 on the New European Bauhaus. 2022. Available online: <https://policycommons.net/artifacts/11156998/european-parliament-resolution-of-14-september-2022-on-the-new-european-bauhaus-20212255ini/12035769/> (accessed on 30 October 2023).
5. Bledzki, A. Composites Reinforced with Cellulose Based Fibres. *Prog. Polym. Sci.* **1999**, *24*, 221–274. [CrossRef]
6. Elfaleh, I.; Abbassi, F.; Habibi, M.; Ahmad, F.; Guedri, M.; Nasri, M.; Garnier, C. A Comprehensive Review of Natural Fibers and Their Composites: An Eco-Friendly Alternative to Conventional Materials. *Results Eng.* **2023**, *19*, 101271. [CrossRef]
7. Guo, A.; Sun, Z.; Feng, H.; Shang, H.; Sathitsuksanoh, N. State-of-the-Art Review on the Use of Lignocellulosic Biomass in Cementitious Materials. *Sustain. Struct.* **2023**, *3*, 000023. [CrossRef]
8. Väisänen, T.; Haapala, A.; Lappalainen, R.; Tomppo, L. Utilization of Agricultural and Forest Industry Waste and Residues in Natural Fiber-Polymer Composites: A Review. *Waste Manag.* **2016**, *54*, 62–73. [CrossRef]
9. Lisboa, F.J.N.; Scatolino, M.V.; de Paula Protásio, T.; Júnior, J.B.G.; Marconcini, J.M.; Mendes, L.M. Lignocellulosic Materials for Production of Cement Composites: Valorization of the Alkali Treated Soybean Pod and Eucalyptus Wood Particles to Obtain Higher Value-Added Products. *Waste Biomass Valorization* **2020**, *11*, 2235–2245. [CrossRef]
10. Amziane, S.; Collet, F.; Lawrence, M.; Magniont, C.; Picandet, V.; Sonebi, M. Recommendation of the RILEM TC 236-BBM: Characterisation Testing of Hemp Shiv to Determine the Initial Water Content, Water Absorption, Dry Density, Particle Size Distribution and Thermal Conductivity. *Mater. Struct./Mater. Constr.* **2017**, *50*, 167. [CrossRef]

11. Diquélou, Y.; Gourlay, E.; Arnaud, L.; Kurek, B. Impact of Hemp Shiv on Cement Setting and Hardening: Influence of the Extracted Components from the Aggregates and Study of the Interfaces with the Inorganic Matrix. *Cem. Concr. Compos.* **2015**, *55*, 112–121. [CrossRef]
12. Liu, Z.; Han, C.; Li, Q.; Li, X.; Zhou, H.; Song, X.; Zu, F. Study on Wood Chips Modification and Its Application in Wood-Cement Composites. *Case Stud. Constr. Mater.* **2022**, *17*, e01350. [CrossRef]
13. Batool, F.; Islam, K.; Cakiroglu, C.; Shahriar, A. Effectiveness of Wood Waste Sawdust to Produce Medium- to Low-Strength Concrete Materials. *J. Build. Eng.* **2021**, *44*, 103237. [CrossRef]
14. Magniont, C.; Escadeillas, G. Chemical Composition of Bio-Aggregates and Their Interactions with Mineral Binders. In *Bio-Aggregates Based Building Materials*; Springer: Dordrecht, The Netherlands, 2017; Volume 23, pp. 1–37.
15. De Castro, V.G. *Compósitos Madeira-Cimento: Um Produto Sustentável Para o Futuro*; EdUFERSA: Mossoró, Brazil, 2021; ISBN 9786587108612.
16. Prusty, J.K.; Patro, S.K.; Basarkar, S.S. Concrete Using Agro-Waste as Fine Aggregate for Sustainable Built Environment—A Review. *Int. J. Sustain. Built Environ.* **2016**, *5*, 312–333. [CrossRef]
17. Jiang, D.; Jiang, D.; Lv, S.; Cui, S.; Sun, S.; Song, X.; He, S.; Zhang, J. Effect of Modified Wheat Straw Fiber on Properties of Fiber Cement-Based Composites at High Temperatures. *J. Mater. Res. Technol.* **2021**, *14*, 2039–2060. [CrossRef]
18. Ataie, F. Influence of Rice Straw Fibers on Concrete Strength and Drying Shrinkage. *Sustainability* **2018**, *10*, 2445. [CrossRef]
19. Danso, H. Effect of Rice Husk on the Mechanical Properties of Cement-Based Mortar. *J. Inst. Eng. Ser. D* **2020**, *101*, 205–213. [CrossRef]
20. Demirbaş, A.; Aslan, A. Effects of Ground Hazelnut Shell, Wood, and Tea Waste on the Mechanical Properties of Cement. *Cem. Concr. Res.* **1998**, *28*, 1101–1104. [CrossRef]
21. Da Costa Santos, A.C.; Archbold, P. Suitability of Surface-Treated Flax and Hemp Fibers for Concrete Reinforcement. *Fibers* **2022**, *10*, 101. [CrossRef]
22. Page, J.; Khadraoui, F.; Gomina, M.; Boutouil, M. Hydration of Flax Fibre-Reinforced Cementitious Composites: Influence of Fibre Surface Treatments. *Eur. J. Environ. Civ. Eng.* **2022**, *26*, 5798–5820. [CrossRef]
23. Pickering, K.L.; Efenidy, M.G.A.; Le, T.M. A Review of Recent Developments in Natural Fibre Composites and Their Mechanical Performance. *Compos. Part A Appl. Sci. Manuf.* **2016**, *83*, 98–112. [CrossRef]
24. Burrows, V.D. Hullless Oat Development, Applications, and Opportunities. In *Oats: Chemistry and Technology*, 2nd ed.; Elsevier Inc.: Amsterdam, The Netherlands, 2011; pp. 31–50. ISBN 9780128104521.
25. Food and Agriculture Organization of the United Nations. Available online: <https://www.fao.org/faostat/en/#data/QCL> (accessed on 8 January 2024).
26. Hackett, R. A Comparison of Husked and Naked Oats under Irish Conditions. *Ir. J. Agric. Food Res.* **2018**, *57*, 1–8. [CrossRef]
27. Bonifacio, A.L.; Archbold, P. The Effect of Calcination Conditions on Oat Husk Ash Pozzolanic Activity. *Mater. Today Proc.* **2022**, *65*, 622–628. [CrossRef]
28. Ruviaro, A.S.; dos Santos Lima, G.T.; Silvestro, L.; Barraza, M.T.; Rocha, J.C.; de Brito, J.; Gleize, P.J.P.; Pelisser, F. Characterization and Investigation of the Use of Oat Husk Ash as Supplementary Cementitious Material as Partial Replacement of Portland Cement: Analysis of Fresh and Hardened Properties and Environmental Assessment. *Constr. Build. Mater.* **2023**, *363*, 129762. [CrossRef]
29. Martínez-Toledo, C.; Valdés-Vidal, G.; Calabi-Floody, A.; González, M.E.; Reyes-Ortiz, O. Effect of Biochar from Oat Hulls on the Physical Properties of Asphalt Binder. *Materials* **2022**, *15*, 7000. [CrossRef]
30. Gil Giraldo, G.A.; Mantovan, J.; Marim, B.M.; Kishima, J.O.F.; Mali, S. Surface Modification of Cellulose from Oat Hull with Citric Acid Using Ultrasonication and Reactive Extrusion Assisted Processes. *Polysaccharides* **2021**, *2*, 218–233. [CrossRef]
31. Varanda, L.D.; do Nascimento, M.F.; Christoforo, A.L.; Silva, D.A.L.; Lahr, F.A.R. Oat Hulls as Addition to High Density Panels Production. *Mater. Res.* **2013**, *16*, 1355–1361. [CrossRef]
32. Wang, L.; Lenorm, H.; Zmamou, H.; Leblanc, N. Effect of Soluble Components from Plant Aggregates on the Setting of the Lime-Based Binder. *J. Renew. Mater.* **2019**, *7*, 903–913. [CrossRef]
33. Welch, R.W.; Hayward, M.V.; Jones, D.I.H. The Composition of Oat Husk and Its Variation Due to Genetic and Other Factors. *J. Sci. Food Agric.* **1983**, *34*, 417–426. [CrossRef]
34. Schmitz, E.; Nordberg Karlsson, E.; Adlercreutz, P. Warming Weather Changes the Chemical Composition of Oat Hulls. *Plant Biol.* **2020**, *22*, 1086–1091. [CrossRef]
35. Kochova, K.; Schollbach, K.; Gauvin, F.; Brouwers, H.J.H. Effect of Saccharides on the Hydration of Ordinary Portland Cement. *Constr. Build. Mater.* **2017**, *150*, 268–275. [CrossRef]
36. Bullard, J.W.; Jennings, H.M.; Livingston, R.A.; Nonat, A.; Scherer, G.W.; Schweitzer, J.S.; Scrivener, K.L.; Thomas, J.J. Mechanisms of Cement Hydration. *Cem. Concr. Res.* **2011**, *41*, 1208–1223. [CrossRef]
37. John, E.; Lothenbach, B. Cement Hydration Mechanisms through Time—A Review. *J. Mater. Sci.* **2023**, *58*, 9805–9833. [CrossRef]
38. Aggarwal, L.K.; Singh, J. Effect of Plant Fibre Extractives on Properties of Cement. *Cem. Concr. Compos.* **1990**, *12*, 103–108. [CrossRef]
39. Vaickelionis, G.; Vaickelioniene, R. Cement Hydration in the Presence of Wood Extractives and Pozzolan Mineral. *Ceram. Silik.* **2006**, *50*, 115–122.

40. Young, J.F. A Review of the Mechanisms of Set-Retardation in Portland Cement Pastes Containing Organic Admixtures. *Cem. Concr. Res.* **1972**, *2*, 415–433. [[CrossRef](#)]
41. *BS EN 197-1*; Cement Composition, Specifications and Conformity Criteria for Common Cements. British Standards Institution: Loughborough, UK, 2011.
42. *BS EN 13139*; Aggregates for Mortar. British Standards Institute: Loughborough, UK, 2013.
43. Rietveld, H.M. A Profile Refinement Method for Nuclear and Magnetic Structures. *J. Appl. Crystallogr.* **1969**, *2*, 65–71. [[CrossRef](#)]
44. Santos Nobre, T.R.; González Pérez, M.; Carlos Bloise, A., Jr.; Cirelli Ângulo, S.; Ota, S.; Angelo Quarcioni, V. Caracterização de Fases de Cimento Portland Por Meio Das Técnicas de Difractometria de Raios X e Espectroscopia de Ressonância Magnética Nuclear de ²⁹Si No Estado Sólido. *Rev. Ipt. Tecnol. Inov.* **2022**, *6*, 67–88. [[CrossRef](#)]
45. *TAPPI T 222 om-02*; Acid-Insoluble Lignin in Wood and Pulp, Test Method T 222 Om-02. Technical Association of the Pulp and Paper Industry: Peachtree Corners, GA, USA, 2002.
46. *ASTM D1110-21*; Standard Test Methods for Water Solubility of Wood. American Society for Testing and Materials: West Conshohocken, PA, USA, 2021.
47. David, S. Etudes Des Interactions Physico-Chimiques Aux Interfaces Fibres de Chanvre/Ciment: Influence Sur Les Propriétés Mécaniques Du Composite. Ph.D. Thesis, Université de Limoges, Limoges, France, 2007.
48. *BS EN 196-3*; Methods of Testing Cement—Part 3: Determination of Setting Times and Soundness. British Standards Institution: Loughborough, UK, 2016.
49. Deboucha, W.; Leklou, N.; Khelidj, A.; Oudjit, M.N. Hydration Development of Mineral Additives Blended Cement Using Thermogravimetric Analysis (TGA): Methodology of Calculating the Degree of Hydration. *Constr. Build. Mater.* **2017**, *146*, 687–701. [[CrossRef](#)]
50. Pane, I.; Hansen, W. Investigation of Blended Cement Hydration by Isothermal Calorimetry and Thermal Analysis. *Cem. Concr. Res.* **2005**, *35*, 1155–1164. [[CrossRef](#)]
51. *BS EN 196-1*; Methods of Testing Cement Part 1: Determination of Strength. British Standards Institution: Loughborough, UK, 2016.
52. ACI Committee 214. *Guide to Evaluation of Strength Test Results of Concrete*; American Concrete Institute: Farmington Hills, MI, USA, 2011.
53. Toby, B.H. R Factors in Rietveld Analysis: How Good Is Good Enough? *Powder Diffr.* **2006**, *21*, 67–70. [[CrossRef](#)]
54. Neitzel, N.; Eder, M.; Hosseinpourpia, R.; Walther, T.; Adamopoulos, S. Chemical Composition, Particle Geometry, and Micro-Mechanical Strength of Barley Husks, Oat Husks, and Wheat Bran as Alternative Raw Materials for Particleboards. *Mater. Today Commun.* **2023**, *36*, 106602. [[CrossRef](#)]
55. Krishnarao, R.V.; Subrahmanyam, J.; Jagadishkumar, T. Preparation of Black Amorphous Silica from Rice Husks. *Trans. Indian Ceram. Soc.* **2001**, *60*, 95–99. [[CrossRef](#)]
56. Chauhan, K.; Sharma, K.; Dutt, B. Variation in Hot and Cold Water Soluble Extractive Content in Gymnosperms from Western Himalayas. *J. Pharmacogn. Phytochem.* **2020**, *9*, 1151–1154. [[CrossRef](#)]
57. Utepov, Y.; Tulebekova, A.; Aldungarova, A.; Mkilima, T.; Zharassov, S.; Shakhmov, Z.; Bazarbayev, D.; Tolkyrbayev, T.; Kaliyeva, Z. Investigating the Influence of Initial Water PH on Concrete Strength Gain Using a Sensors and Sclerometric Test Combination. *Infrastructures* **2022**, *7*, 159. [[CrossRef](#)]
58. Bishop, M.; Barron, A.R. Cement Hydration Inhibition with Sucrose, Tartaric Acid, and Lignosulfonate: Analytical and Spectroscopic Study. *Ind. Eng. Chem. Res.* **2006**, *45*, 7042–7049. [[CrossRef](#)]
59. Mollah, M.Y.A.; Yu, W.; Schennach, R.; Cocke, D.L. A Fourier Transform Infrared Spectroscopic Investigation of the Early Hydration of Portland Cement and the Influence of Sodium Lignosulfonate. *Cem. Concr. Res.* **2000**, *30*, 267–273. [[CrossRef](#)]
60. Ylmén, R.; Jäglid, U. Carbonation of Portland Cement Studied by Diffuse Reflection Fourier Transform Infrared Spectroscopy. *Int. J. Concr. Struct. Mater.* **2013**, *7*, 119–125. [[CrossRef](#)]
61. Delgado, A.H.; Paroli, R.M.; Beaudoin, J.J. Comparison of IR Techniques for the Characterization of Construction Cement Minerals and Hydrated Products. *Appl. Spectrosc.* **1996**, *50*, 970–976. [[CrossRef](#)]
62. Collier, N.C. Transition and Decomposition Temperatures of Cement Phases—A Collection of Thermal Analysis Data. *Ceram.-Silik.* **2016**, *60*, 338–343. [[CrossRef](#)]
63. Aprianti, E.; Shafiqh, P.; Bahri, S.; Farahani, J.N. Supplementary Cementitious Materials Origin from Agricultural Wastes—A Review. *Constr. Build. Mater.* **2015**, *74*, 176–187. [[CrossRef](#)]
64. *ASTM C511-03*; Standard Specification for Mixing Rooms, Moist Cabinets, Moist Rooms, and Water Storage Tanks Used in the Testing of Hydraulic Cements and Concretes. American Society for Testing and Materials: West Conshohocken, PA, USA, 2017.

Disclaimer/Publisher’s Note: The statements, opinions and data contained in all publications are solely those of the individual author(s) and contributor(s) and not of MDPI and/or the editor(s). MDPI and/or the editor(s) disclaim responsibility for any injury to people or property resulting from any ideas, methods, instructions or products referred to in the content.